Chapter VI

Phosphate Adsorption onto TPVSP and TBVSP

Employment of TPVSP and TBVSP in the removal of phosphate ions from aqueous solutions had been verified and explained in this chapter.

6.1 Scanning Electron Microscopy/ EDAX studies

Surface morphological changes with smooth covering of texture in figure 6.1 (b) against the ruggedness exhibited by 6.1 (a) support the sorption of PO_4^{3-} onto TPVSP and TBVSP as derived from SEM images. Figures 6.3 and 6.4 correspond to the EDAX spectra of phosphate laden sorbent materials. Presence of peaks at 2 keV confirm that, phosphate sorption had occurred at the sorbents' surfaces.
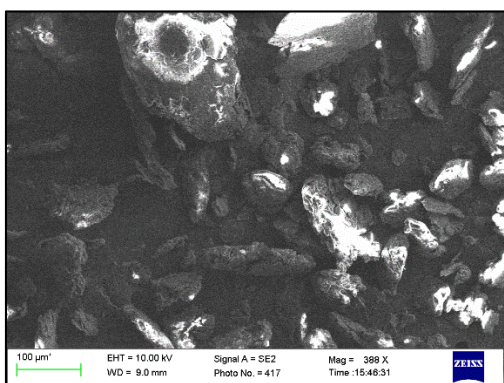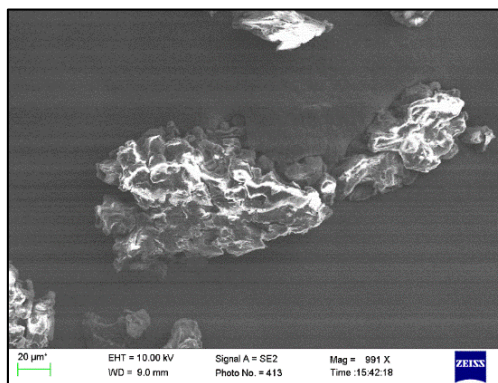

Figure 6.1 (a) SEM- Unloaded TPVSP
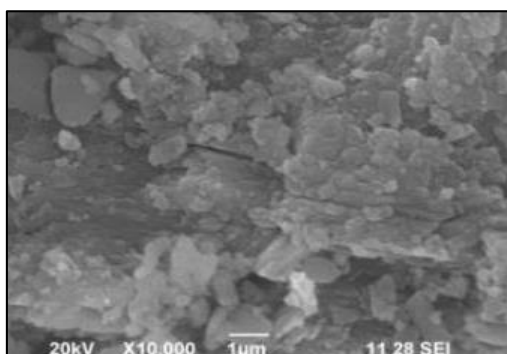

Figure 6.1 (b) SEM- PO_4^{3-} - TPVSP

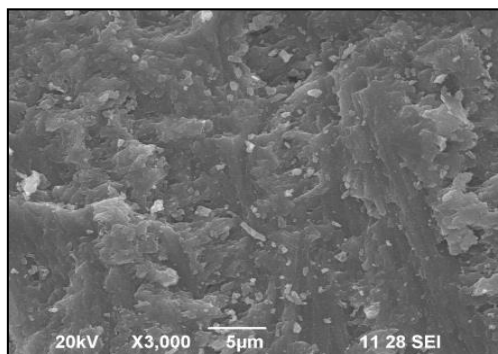**Figure 6.2 (a) SEM- Unloaded TBVSP**

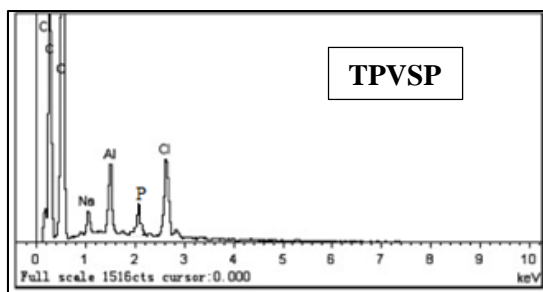**Figure 6.2 (b) SEM- PO_4^{3-}-TBVSP**
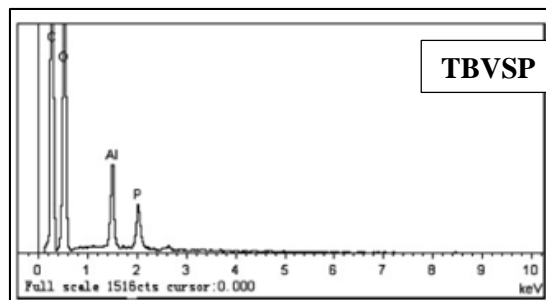
Figure 6.3 EDAX -Phosphate -TPVSP   **Figure 6.4 EDAX -Phosphate - TBVSP**

6.2. Batch Equilibration Studies

6.2.1 Effect of Particle Size

The sorption rate of phosphate upon TPVSP and TBVSP at varying particle sizes are listed in table 6.1 and the corresponding data are depicted in figure 6.5. It is clear from the figure that, maximum amount of PO_4^{3-} sorption had occurred at 0.18 mm, further degradation of the curve at higher particle sizes is obvious. 0.18 mm, being the smaller particle size employed in the current study, exhibits maximum uptake of PO_4^{3-} ions, emphasizing the fact that it possesses larger surface area[1]. Based on these results, 0.18 mm particle size is considered as the optimum concentration for further experiments.

Table 6.1 Effect of Particle Size

Percentage Removal (%)		
Particle Size (mm)	**TPVSP**	**TBVSP**
0.18	98.25	97.54
0.24	82.34	78.42
0.3	74.45	65.64
0.42	64.95	55
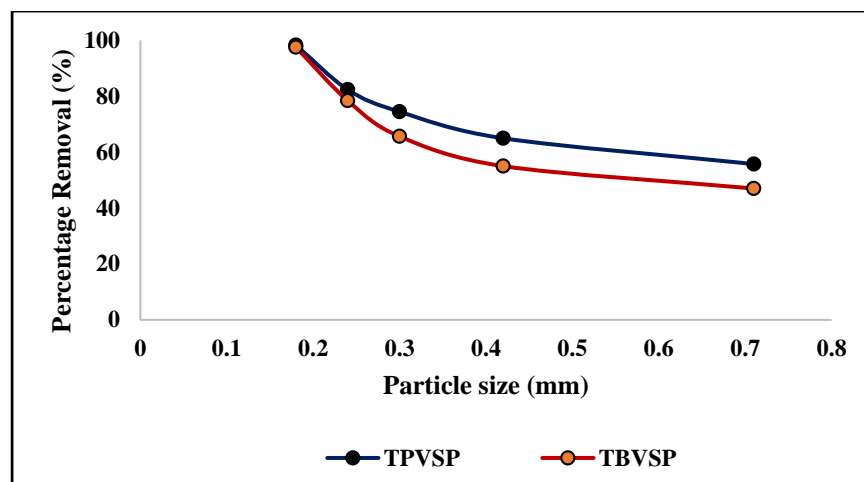
Figure 6.5 Effect of Particle Size

6.2.2 Effect of Initial Phosphate Concentration/ Contact time

Table 6.2 refer to the removal of the trivalent anion by the treated shell powders at varying concentrations and pre-set time schemes. Figures 6.6 (a) and (b) derived from the tabulated data reveal that remarkable sorption had occurred at a minimum contact time of 10 minutes with a maximum phosphate removal (99 %), the curve trends being atop for 10 mg/L against higher concentrations. This may be due to the fact of rapid initial uptake rate and overlapping of adsorption sites after the equilibrium point. Thence, 10 mg/L and 10 minutes were decided as the controlling factors in the forthcoming experiments.

Table 6.2 Effect of Initial concentration & Contact time

Adsorbent	Time (mins)	Percentage Removal (%)				
		5 mg/L	10mg/L	15 mg/L	20 mg/L	25 mg/L
TPVSP	0	0	0	0	0	0
	5	68	88	55	49	36
	10	80	99	53	50	38
	15	70	85	50	45	34
	20	74	78	48	42	30
	25	70	72	45	38	35
	30	64	68	42	34	22

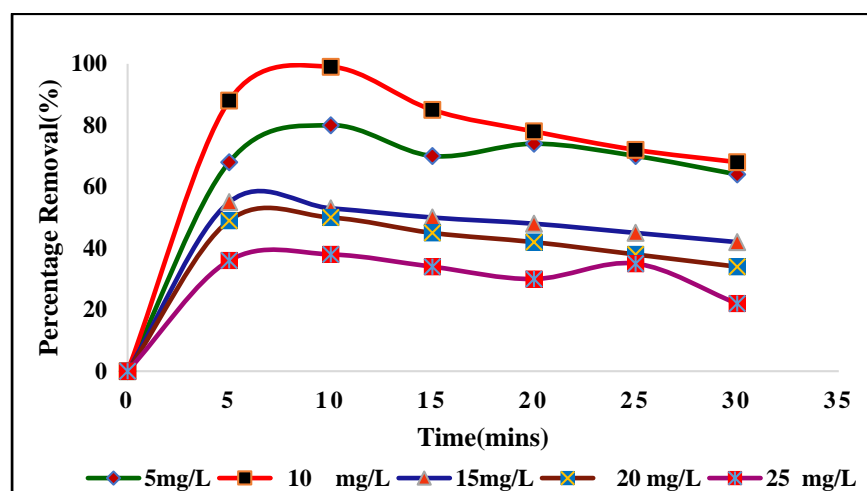| Adsorbent	Time (mins)	Percentage Removal (%)				
		5 mg/L	**10mg/L**	**15 mg/L**	**20 mg/L**	**25 mg/L**
TBVSP	0	0	0	0	0	0
	5	32	80	69	55	49
	10	31	99	78	53	50
	15	30	85	69	50	45
	20	34	78	65	48	42
	25	30	72	63	45	38
	30	28	68	62	42	34

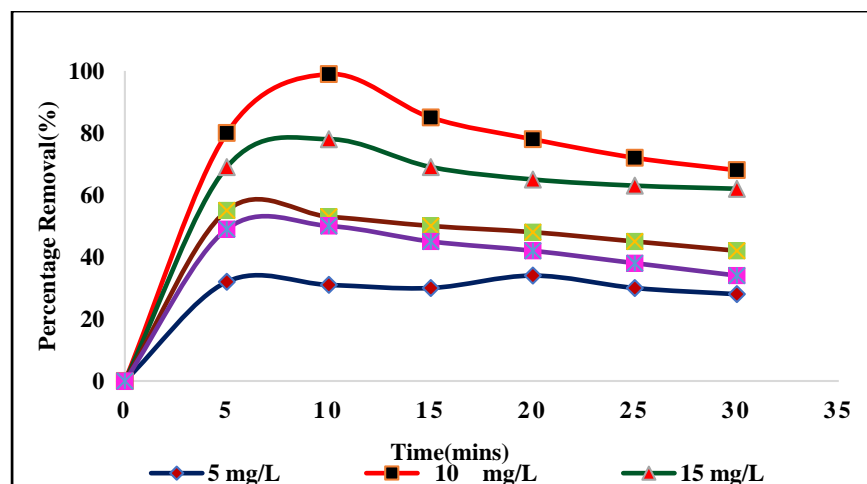**Figure 6.6 (a) Effect of Initial Concentration & Contact time (TPVSP)**

Figure 6.6 (b) Effect of Initial Concentration & Contact Time (TBVSP)

6.2.3 Effect of Dosage

The influence of different doses (TPVSP/ TBVSP) for the removal of PO_4^{3-} ions is given in table 6.3 and the inclined curves followed by a mere saturation pertaining to tabulated values are illustrated in figures 6.7 (a) and (b). Approximately 99 % of anionic removal is seen from the graph for 100 mg. A marked escalation in the percentage removal at higher dosages could be due to a greater number of active sites[2]. Thereby, the latter is fixed as the sorbent dosage.

Table 6.3 Effect of Dosage

Percentage Removal (%)				
TPVSP				
Time	10 mg	25 mg	50 mg	75 mg	100 mg
5	32.9	40.3	65.1	78.5	79.2
10	34.4	42.5	67.5	74.0	80.7
15	34.1	44.1	66.2	73.7	79.5
20	35.2	40.5	67.8	72.1	78.1
25	35.1	37.0	65.1	70.0	75.5
30	34.9	37.5	68.5	72.3	65.7

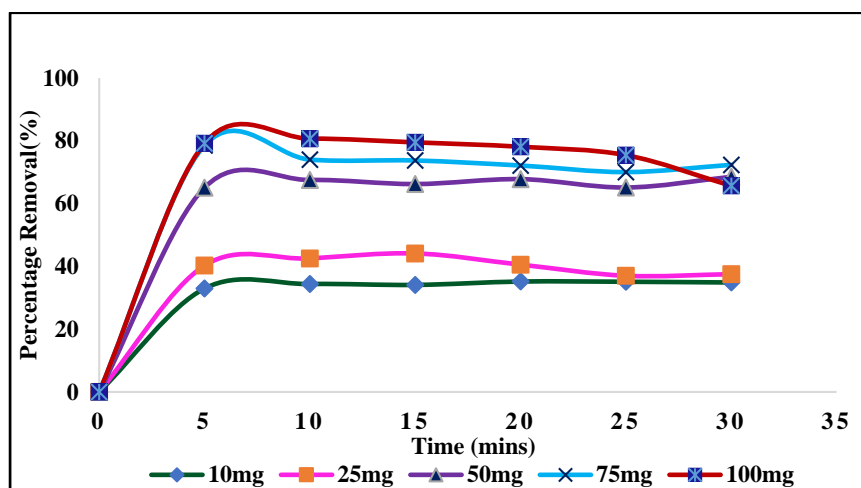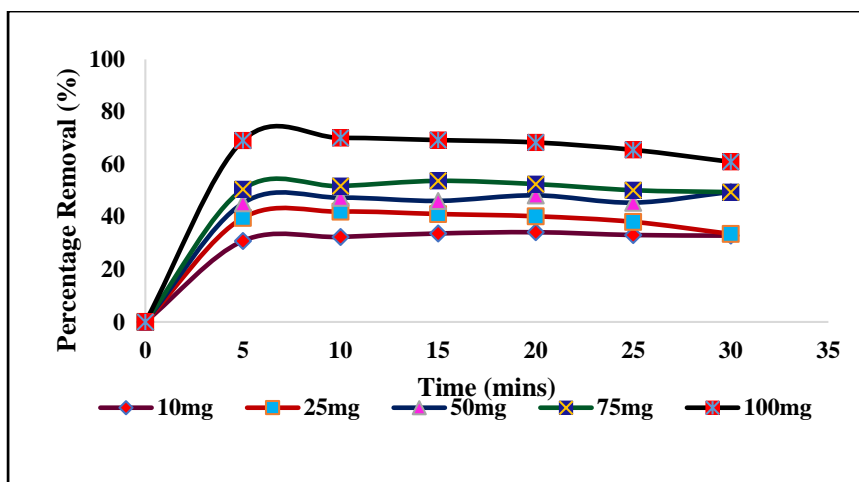| Percentage Removal (%)				
TBVSP				
Time	**10 mg**	**25 mg**	**50 mg**	**75 mg**	**100 mg**
5	30.9	39.6	45.2	50.5	69.1
10	32.4	42	47.3	51.7	70.1
15	33.7	41.1	46.1	53.7	69.3
20	34.2	40.2	48.2	52.5	68.4
25	33.1	38.1	45.4	50.2	65.6
30	32.9	33.5	49.5	49.5	60.9

Figure 6.7 (a) Effect of Dosage (TPVSP)

Figure 6.7 (b) Effect of Dosage (TBVSP)

6.2.4 Effect of pH

The data obtained for phosphate removal at different pH environments for both PO_4^{3-}-TPVSP and PO_4^{3-}-TBVSP systems are depicted in figures 6.8 (a) and (b). Appearance of approximate inverted parabolas for both the systems with maximum inversion at pH 6.5 and 7.5 justify the extensive adsorption at this pH. Declined removal at acidic range may be attributed to the involvement of binding nature of phosphate ions i.e., formation of $H_2PO_4^{-}$ and HPO_4^{2-}. Also, a reduction in the binding capacity of PO_4^{3-} at alkaline medium, support the statement where OH^- ions get preferentially sorbed on TPVSP and TBVSP surfaces [4]. The above observations are in good agreement with Benyoucef, S., & Amrani, M [5].
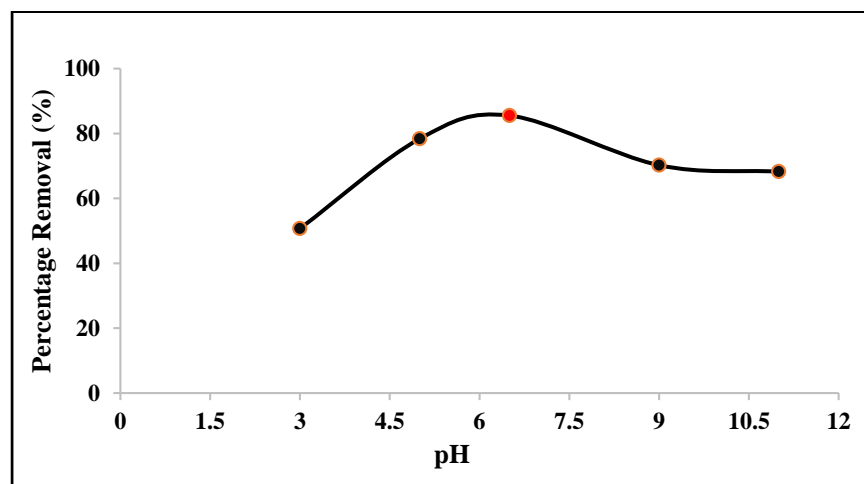

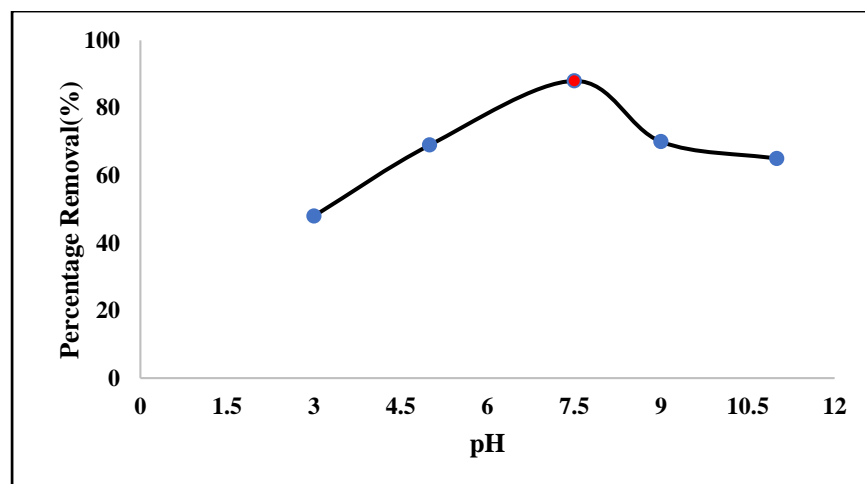**Figure 6.8 (a) Effect of pH (TPVSP)**

Figure 6.8 (b) Effect of pH (TPVSP)

6.2.5 Effect of Temperature

The influence of temperature tap holds to be an important factor in the adsorption process. Temperature rise [6] from 293K to 323K leads to direct proportion of sorption rate. It is evident from figure 6.9, that the adsorption capacities of TPVSP and TBVSP against phosphate ion exhibited marginal increase of almost 99 % removal at 303 K.

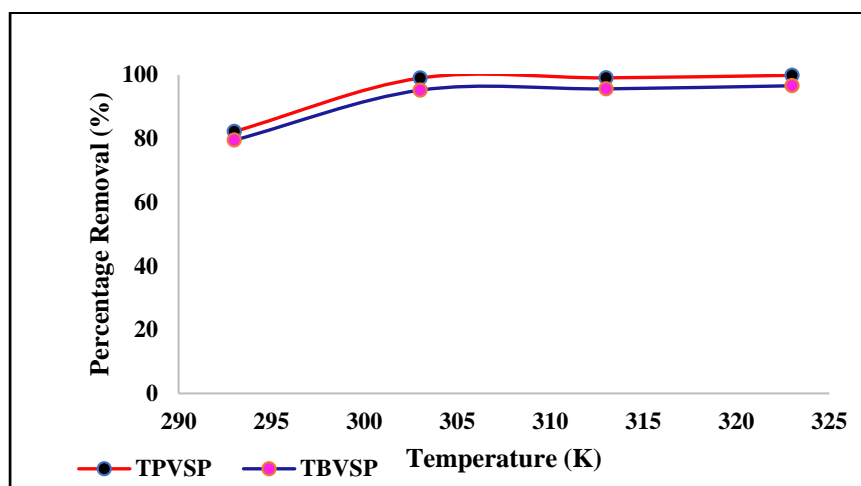**Figure 6.9 Effect of Temperature (PO_4^{3-} TPVSP/ TBVSP)**

6.2.6 Effect of Co-existing Ions

Sorption capacities of TPVSP and TBVSP onto the trivalent anion were carried out by binary coexisting ions viz., fluorides, chlorides and sulphates (Table 6.4). Fluoride and chloride ions exhibit marked influence. However, SO_4^{2-} had registered a comparatively

minimal inhibitive property, this shall be due to the electronegative character[7] of the specific anion. The figures evidenced in figure 6.10, are in good agreement with S. Meenakshi et., al [8] in the removal of nitrate and phosphate anions using amine modified chitosan beads.

Table 6.4 Effect of Co-existing Ions

Adsorbents	PO_4^{3-} in the absence of ions	Percentage Removal (%)		
		F^-	Cl^-	SO_4^{2-}
TPVSP	99.3	54.2	53.6	65.7
TBVSP	99.0	45.6	44.5	60.0
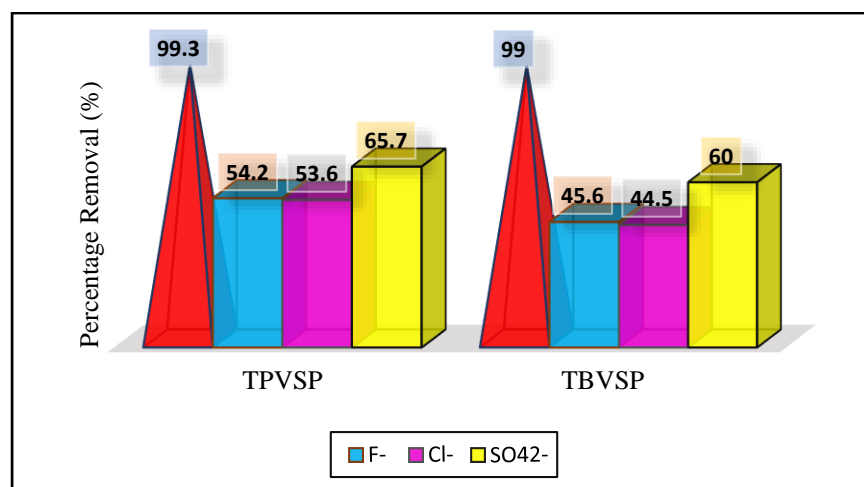
Figure 6.10 Effect of Co-existing ions

6.3 Isothermal Studies

Langmuir, Freundlich and Dubinin-Kaganer-Radushkevich isothermal reckonings plotted using the data (table 6.5) confirm the linear fit for the twin systems (PO_4^{3-}-TPVSP/TBVSP). The derived isothermal constants from the respective plots and equilibrium factors are summarized in tables 6.6 & 6.7, followed by the further discussions.

Table 6.5 Equilibrium Concentrations − Isothermal Data

Systems	Conc. of Metal Ion	Langmuir		Freundlich		DKR	
	(mg/L)	C_e	C_e/q_e	log C_e	log q_e	ε^2*10^{-5}	ln q_e
PO_4^{3-} TPVSP	5	1.09	0.56	0.04	0.29	26.90	0.97
	10	1.05	0.66	0.02	0.41	28.41	1.18
	15	6.51	1.43	0.81	0.63	5.12	1.45
	20	10.28	2.12	1.01	0.69	0.55	1.58
	25	15.38	2.99	1.19	0.68	0.25	1.57
PO_4^{3-} TBVSP	5	1.24	0.26	0.09	0.65	22.20	1.23
	10	1.90	0.47	0.28	0.61	11.35	1.40
	15	3.27	0.56	0.51	0.71	5.12	1.77
	20	9.32	1.75	0.97	0.77	0.66	1.68
	25	12.48	2.18	1.10	0.80	0.38	1.83

Table 6.6 Isothermal Constants

Systems	Langmuir			Freundlich			DKR		
	q_m (mg/g)	b (L/g)	R^2	K_F (mg/g)	1/n	R^2	q_s (mg/g)	E (KJ/mol)	R^2
PO_4^{3-} TPVSP	6.02	0.4	0.9973	2.23	3.21	0.9208	4.79	5.29	0.8963
PO_4^{3-} TBVSP	5.8	2.45	0.994	4.03	5.83	0.8733	5.99	4.4	0.8696

6.3.1 Langmuir Model

A plot of C_e / q_e vs C_e (Figures 6.11 & 6.12) for phosphate system shows a straight line, indicative of monolayer process of adsorption. This is confirmed by b and R_L data being less than unity (Tables 6.7)
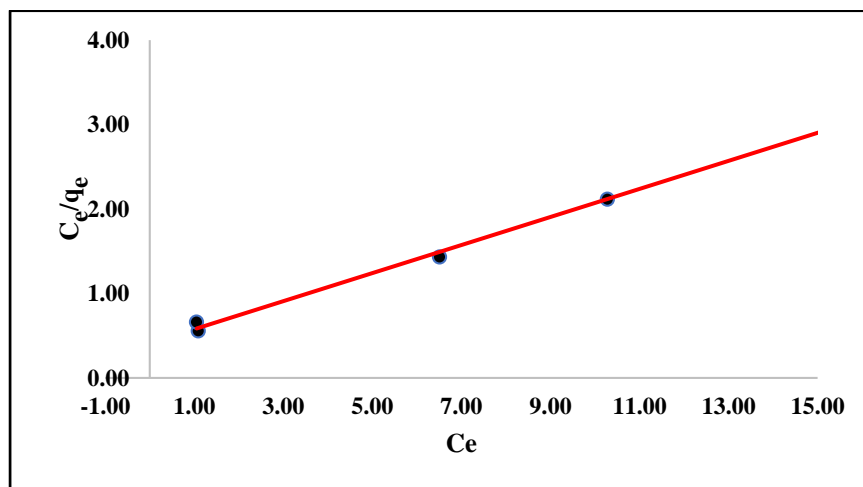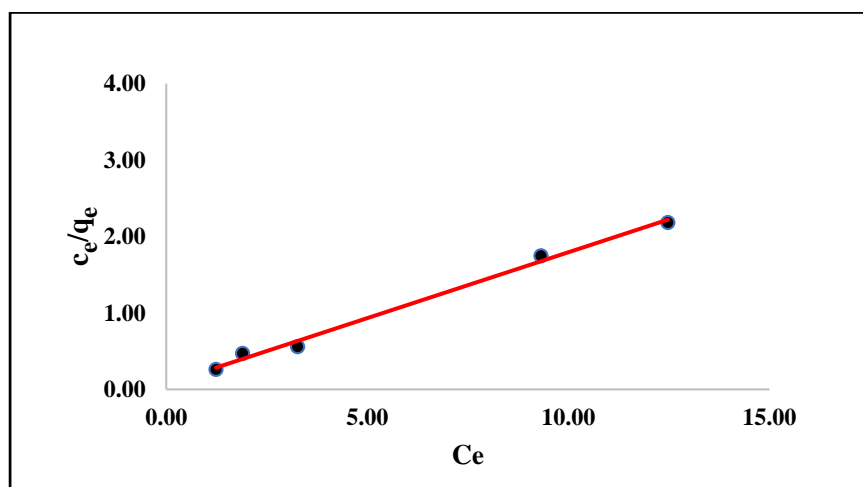

Figure 6.11 Langmuir Plot TPVSP

Figure 6.12 Langmuir Plot TBVSP

Table 6.7 Equilibrium Parameter (R_L)

Conc. (mg/L)	PO_4^{3-}- TPVSP	PO_4^{3-}- TBVSP
5	0.33	0.08
10	0.20	0.04
15	0.14	0.03
20	0.11	0.02
25	0.09	0.02

6.3.2 Freundlich Model

Values of sorption intensity in the range of $0 < 1/n < 1$ as evidenced from Freundlich plots (Figures 6.13 & 6.14) suggest the model to be beneficial. In other words, R^2 values are comparatively lesser for this model, (due to certain dislocation of the points in the graphs) than Langmuir, thereby implying Freundlich Model to be less applicable.
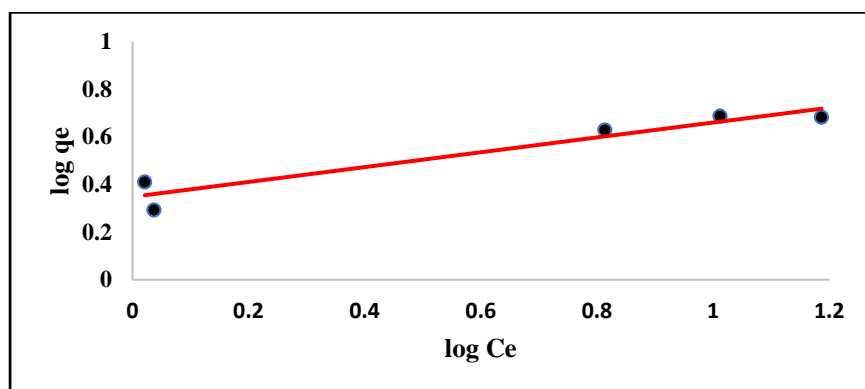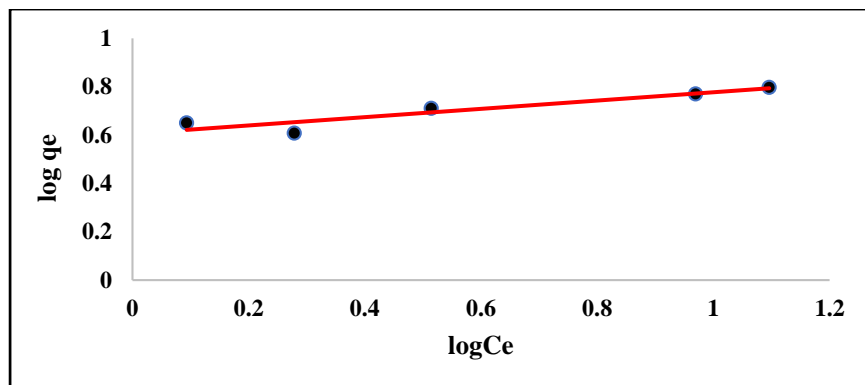

Figure 6.13 Freundlich Plot TPVSP

Figure 6.14 Freundlich Plot TBVSP

6.3.4 Dubinin–Kaganer-Radushkevich Model

DKR constant q_s and E were calculated from the plots ln qe vs ε^2 (Figure 6.15 & 6.16) for trivalent phosphate using TPVSP/TBVSP. The mean free energy values being less than 8 KJ/ mol, favour the mechanism to be physisorption[13].
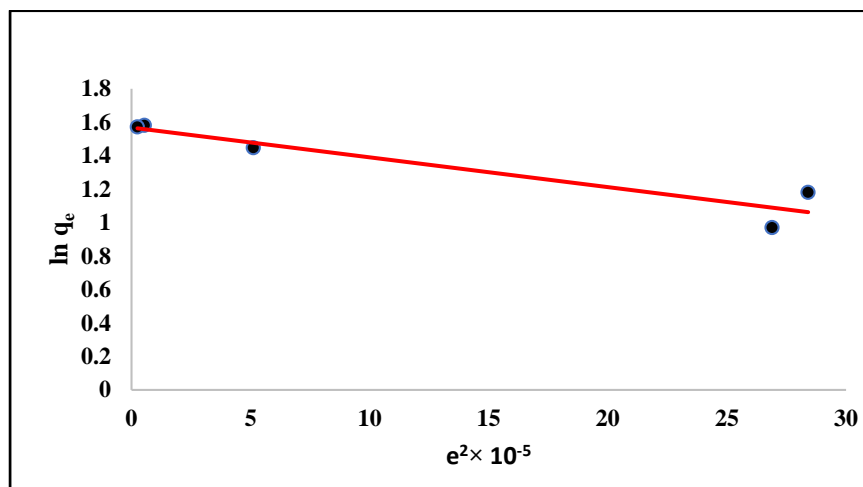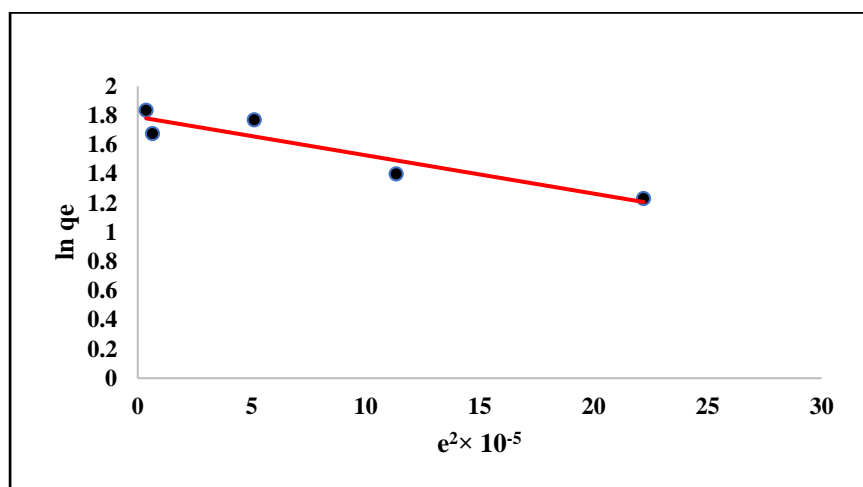

Figure 6.15 DKR Plot (TPVSP)

Figure 6.16 DKR Plot (TBVSP)

Similar to previous isothermal discussions, the favourable order for PO_4^{3-} system is also Langmuir> Freundlich> DKR.

6.4 Adsorption Dynamics

Thermodynamic parameters $\Delta G°$, $\Delta H°$ and $\Delta S°$ calculated from the slopes and intercepts of Van't Hoff 's plots (Figures 6.17 & 6.18) expressed as ln K_c vs 1/T is shown in table 6.8. These values were similar to that of Pb(II) systems, the reactions observed to be spontaneous, endothermic and notably random. [17-18]
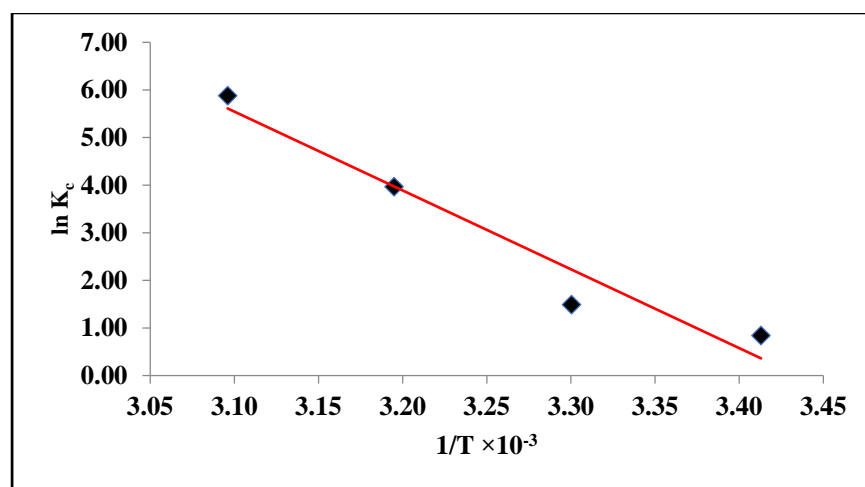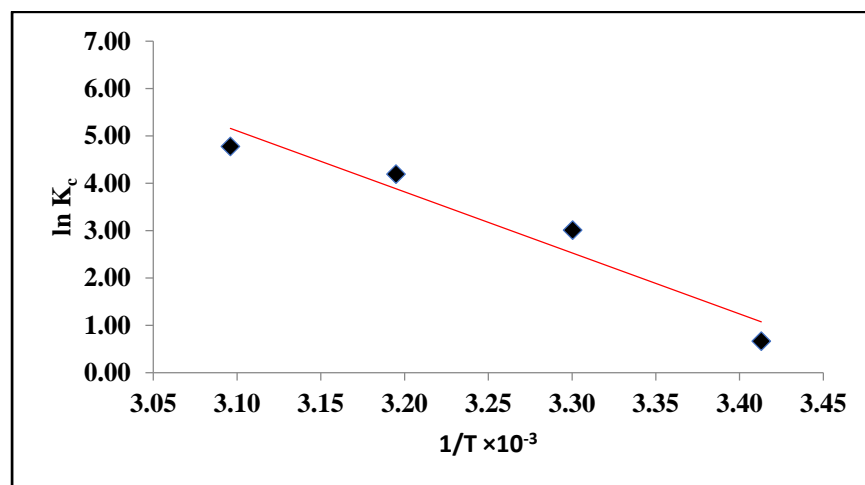

Figure 6.17 Van't Hoff's Plot (TPVSP)

Figure 6.18 Van't Hoff's Plot (TBVSP)

Table 6.8 Thermodynamic Parameters

Temp. (K)	PO_4^{3-} - TPVSP			PO_4^{3-} – TBVSP		
	$\Delta G^\circ X\ 10^{-3}$ (KJ/mol)	ΔH° (KJ/mol)	ΔS° (J/mol K)	$\Delta G^\circ X\ 10^{-3}$ (KJ/mol)	ΔH° (KJ/mol)	ΔS° (J/mol K)
293	-0.2			-0.16		
303	-0.38	16.55	56.86	-0.89	12.89	45.07
313	-1.03			-1.09		
323	-1.58			-1.28		

6.5 Conclusion

Verification of TPVSP and TBVSP (prepared as per previous discussions) was extended to explore its sorptive behaviour towards phosphate ions, due to their acute occurrence in the discharges of battery service centers. Batch equilibration data exhibited a maximum of 99% PO_4^{3-} removal for both the sorbents at 0.18 mm, 100 mg, 10 mg/L PO_4^{3-} ion, 10 mins, pH 6.5/pH 7.5. This was confirmed by the obvious changes in the morphological SEM images and appearance of new EDAX peaks, recorded for PO_4^{3-} loaded precursors against their treated shell powders. Specific inhibition in the uptake of PO_4^{3-} by the materials was noticed under the influence of respective ions. Verification of adsorption isotherm favored phosphate systems to be preferentially fit into Langmuir model. It is concluded that both the chosen materials prove to be promising in sequestering ubiquitous phosphate ion from aqueous media.

6.6 References

1. Dr. M.Jai Paul, Jis Jimmy, M.Josento Therattil, LindaRegi, Shirin Shahana, Removal of Heavy Metals Using Low Cost Adsorbents, *Journal of Mechanical and Civil Engineering,* 14(3),(**2017**),48-50.

2. E. Subha, S. Sasikala, G. Muthuraman, Removal of Phosphate from Wastewater using Natural Adsorbents, *International Journal of Chemical Technology Research,* 7(7), (**2015**), 3095-3099.

3. C. R. Ramakrishnaiah,Vismitha, Removal of Phosphate from Wastewater using Low-Cost Adsorbents, *International Journal of Engineering Inventions,* 1(7), (**2012**), 44-50.

4. E. Oguz, A. Gurses, M. Yalcin, Removal of Phosphate from Waste Water by Adsorption*, WaterAir Soil Pollution,* 148, (**2003**),279–287.

5. S.Benyoucef, M. Amrani, Adsorption of Phosphate Ions onto Low Cost Aleppo Pine Adsorbent, *Desalination*, 275(1-3), (**2011**), 231–236.

6. J.Pradhan Das, J. Das, &S.Thakur, Adsorption of Phosphate from Aqueous Solution Using Activated Red Mud, *Journal of Colloid and Interface Science*, 204(1), (**1998**), 169–172.

7. Ramin Nabizadeh, Mahsa Jahangiri-rad and Mohammad Rafiee, Counterion Effects on Nitrate Adsorption from Aqueous Solution onto Functionalized Polyacrylonitrile Coated with Iron Oxide Nanoparticles, *Research Journal of Environmental Sciences*, 8(5),(**2014**), 287-293.

8. A. Sowmya, S.Meenakshi,An Efficient and Regenerable Quaternary Amine Modified Chitosan Beads for the Removal of Nitrate and Phosphate Anions, *Journal of Environmental Chemical Engineering*, 1(4), (**2013**), 906-915.

9. X.Liu, & L. Zhang, Removal of Phosphate Anions using the Modified Chitosan Beads: Adsorption Kinetic, Isotherm and Mechanism Studies, *Powder Technology*, 277, (**2015**), 112–119.

10. S.D.Mallikarjun, Dr. S.R.Mise, A Study of Phosphate Adsorption Characteristics on Different Soils, *Journal of Engineering,* 2(7), (**2012**), 13-23.

11. Xiaoli Yuan, Wentang Xia, Juan An, Jianguo Yin, Xuejiao Zhou and Wenqiang Yang, Kinetic and Thermodynamic Studies on the Phosphate Adsorption Removal by Dolomite Mineral, *Journal of Chemistry*, (**2015**).

12. K.Vijayaraghavan, T.Padmesh, K.Palanivelu & M.Velan, Biosorption of Ni (II) ions onto *Sargassum wightii:* Application of Two-Parameter and Three-Parameter Isotherm Models. *Journal of Hazardous Materials*, 133(1-3), (**2006**), 304–308.

13. Runping Han, Jinghua Zhang, Weihua Zou, Jie Shi, Hongmin Liu, Equilibrium Biosorption Isotherm for Lead Ion on Chaff, *Journal of Hazardous Materials,* 125, (**2005**)**,** 266-271

14. Rajesh Dandge, Milind Ubaleand Shantilal Rathod. Heavy Metals Removal from Industrial Wastewater by Activated Carbon Prepared from Shell of Green Peas (*Pisum sativum*), *Journal of Medicinal Chemistry and Drug Discovery*, 1(2), (**2016**),210-224.

15. A. Bandyopadhyay and M.N. Biswas, Removal of Hexavalent Chromium by Synergism Modified Adsorption, *Indian Journal of Environmental Protection* 18 (9), (**1998**),662-671.

16. J. Patil, A.G. Bhole, and G.S. Natarajan, Scavenging of Ni (II) Metal Ions by Adsorption on PAC and BabhulBark, *Journal of Environmental Science*, (**2006**), 203-208.

17. M. Tanyol, V.Yonten, &V. Demir, Removal of Phosphate from Aqueous Solutions by Chemical- and Thermal-Modified Bentonite Clay. *Water, Air, & Soil Pollution*, 226(8), (**2015**).

18. Abdel Zaher MS, Abdel Wahab SM, Taha MH and Masoud AM, Sorption Characteristics of Iron, Fluoride and Phosphate from Wastewater of Phosphate Fertilizer Plant using Natural Sodium Bentonite, *Journal Member of Science and Technology,* 8(2), (**2018**), 1-10.